Progress In Electromagnetics Research, PIER 23, 39–58, 1999

ANALYSIS OF ELECTROMAGNETIC WAVE DIFFRACTION BY A SEMI-INFINITE STRIP GRATING AND EVALUATION OF END-EFFECTS

M. Nishimoto and H. Ikuno

Department of Electrical and Computer Engineering
Kumamoto University, Kurokami
Kumamoto 860-8555, Japan

1. INTRODUCTION

In electromagnetic wave theory and optics, the analysis of the diffraction by gratings is a very important problem, and diffraction characteristics of various kinds of gratings have been investigated so far [1–4]. In most of these analyses, it is assumed that the periodic structure of the grating has infinite extent. The actual gratings, however, have finite extent and their diffraction characteristics are different from those of infinite gratings because of the "end-effects" that caused by the ends of the finite gratings. Therefore, the diffraction by finite gratings have also been analyzed and diffraction characteristics have been investigated [5–9]. On the other hand, the most suitable model for analyzing the end-effects of finite gratings is a semi-infinite grating, because it can provide end-effects contributions in pure form as the Sommerfeld's solution for half-plane can provide the information of edge diffraction. However, the analysis of the diffraction by a semi-infinite grating is

much difficult because the Floquet's theorem cannot be applied to it, and there are very few reports about this problem. Hills and Karp [10] have analyzed this problem by using the Wiener-Hopf technique and have revealed the interesting diffraction phenomena. In their analysis, the problem have been solved under the assumption that the thin wire elements are widely spaced relative to the wavelength. However, it is necessary to reveal the diffraction characteristics for narrow spacing in using the finite grating for practical applications such as frequency selective surface or polarization selective surface [11–13].

In this paper, we analyze the diffraction of plane electromagnetic wave by a semi-infinite strip grating and investigate the end-effects contribution. In this analysis we assume that each strip is narrow relative to the wavelength, but there is no restriction in spacing of the strip elements. In the formulation, we divide the current induced on each strip into two currents, the periodic current on the infinite strip grating and the correction current induced by the truncation of the periodic structure. These currents are determined by solving a set of integral equations. (Outline of the formulation were reported in the previous letter [14].) In order to investigate the end-effect contribution, numerical calculations are carried out for current distribution, diffraction patterns, and radiated powers by the induced currents.

2. FORMULATION OF THE PROBLEM

Let us consider a semi-infinite strip grating as shown in Fig. 1(a). The spacing between the strips is d and each strip has a width $2a$. The incident wave is an E-polarized plane wave given by

$$E^i(x,y) = e^{-ik(x\sin\theta_i - y\cos\theta_i)} \tag{1}$$

where θ_i is an incident angle, $k = \omega\sqrt{\varepsilon_0\mu_0} = 2\pi/\lambda$ is a wavenumber, and λ is a wavelength. The current induced on each strip has only a z-component. For convenience, let us divide the current density on the n-th strip $J^h(nd+x)(|x|<a)$ into two parts:

$$J^h(nd+x) = J^p(nd+x) + J^c(nd+x) \qquad |x| \le a, \qquad n = 0,1,2,\cdots \tag{2}$$

where $J^p(nd+x)$ is the current on the infinite strip grating as shown in Fig. 1(b) and $J^c(nd+x)$ is the unknown correction current induced by the removal of the strips located on negative x axis. For periodicity

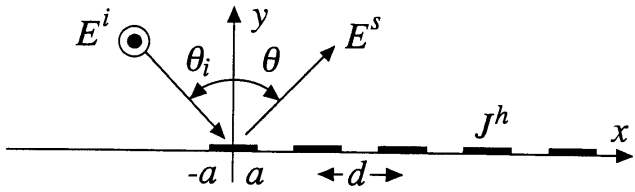

(a) Semi-infinite strip grating

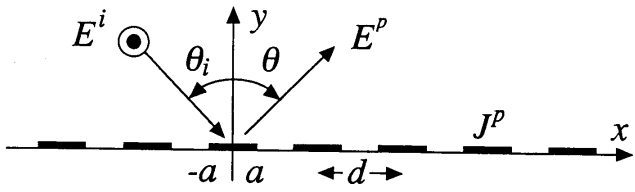

(b) Infinite strip grating

Figure 1. Geometry of the problem.

of the structure, $J^p(nd+x)$ satisfies the following periodic condition

$$J^p(nd+x) = e^{-in\beta_0 d} J^p(x) \tag{3}$$

$$\beta_0 = k\sin\theta_i \tag{4}$$

From physical consideration, it is obvious that $J^h(nd+x)$ approaches $J^p(nd+x)$ as n increases. Therefore, $J^c(nd+x)$ has a following important property:

$$|J^c(nd+x)| \to 0 \qquad \text{as} \qquad n \to \infty \tag{5}$$

The integral representation of the scattered field E^p from an infinite strip grating of Fig. 1(b) has only z component and expressed as follows:

$$E^p(x,y) = -i\omega\mu_0 \sum_{n=-\infty}^{\infty} e^{-in\beta_0 d} \int_{-a}^{a} J^p(x') G(x,y|nd+x',0)dx' \tag{6}$$

where $G(x,y|x',y')$ is the two-dimensional Green's function

$$G(x,y|x',y') = \frac{1}{4i} H_0^{(2)}(k\sqrt{(x-x')^2+(y-y')^2}\,) \tag{7}$$

and $H_0^{(2)}$ is the Hankel function of the second kind. By applying the boundary condition

$$E^i(nd+x,0)+E^p(nd+x,0)=0 \quad \text{for } |x|\le a, \quad n=0,\pm1,\pm2,\cdots \tag{8}$$

to Eq. (6), we can derive the following integral equation for $J^p(x)$.

$$E^i(x,0)=i\omega\mu_0\sum_{n=-\infty}^{\infty}e^{-in\beta_0 d}\int_{-a}^{a}J^p(x')G(x,0|nd+x',0)dx', |x|\le a \tag{9}$$

Similarly, the integral representation of the diffracted field from a semi-infinite strip grating is expressed as

$$E^s(x,y)=-i\omega\mu_0\sum_{n=\infty}^{\infty}\int_{-a}^{a}J^h(nd+x')G(x,y|nd+x',0)\ dx' \tag{10}$$

and the integral equation for $J^c(nd+x)$ is expressed as follows:

$$\begin{aligned}E^i(md+x,0)=&\ i\omega\mu_0\sum_{n=0}^{\infty}e^{-in\beta_o d}\int_{-a}^{a}J^p(x')G(md+x,0|nd+x',0)dx'\\&+i\omega\mu_0\sum_{n=0}^{\infty}\int_{-a}^{a}J^c(nd+x')G(md+x,0|nd+x',0)dx'\\&|x|\le a, \quad m=0,1,2,\cdots\end{aligned} \tag{11}$$

where we use Eqs. (2) and (3). If $J^p(x)$ is obtained by solving Eq. (9), then $J^c(nd+x)$ can be determined by solving Eq. (11).

In order to solve Eqs. (9) and (11), we assume that the strip is narrow relative to the wavelength:

$$2ka << 1 \tag{12}$$

Under the above assumption, the phase of the current on the strip is considered to be constant over the strip, but the amplitude has singularities at the edges of the strip. Taking account of the edge condition, J^p and J^c can be approximated as follows:

$$J^p(x)\approx\frac{2}{\pi}\frac{\overline{J}^p}{\sqrt{1-(x/a)^2}}, \qquad |x|\le a \tag{13}$$

$$J^c(nd+x)\approx\frac{2}{\pi}\frac{\overline{J}^c_n}{\sqrt{1-(x/a)^2}} \qquad |x|\le a, \quad n=0,1,2,\cdots \tag{14}$$

where $\overline{J}^p$ and $\overline{J}^c_n$ are the unknown constants to be determined and they correspond to the averaged current densities on the strips. Since the strip is narrow, both sides of Eqs. (9) and (11) are considered to be constant over the range $|x| \leq a$, and they are approximated by their average values. Taking the average of the both sides of Eqs. (9) and (11) yields

$$\overline{J}^p = \frac{\overline{E}^i_0}{2i\omega\mu_0 a(S_1 + G_0)} \tag{15}$$

and

$$\sum_{n=0}^{\infty} G_{n-m}\overline{J}^c_n = \frac{\overline{E}^i_m}{2i\omega\mu_0 a} - \overline{J}^p e^{-im\beta_0 d}\left(S_2 + \sum_{l=0}^{m} e^{-il\beta_0 d} G_l\right) \tag{16}$$
$$m = 0, 1, 2, \cdots$$

where

$$\overline{E}^i_m = \frac{1}{a}\int_{-a}^{a} E^i(md + x)\, dx \tag{17}$$

$$G_n = \frac{1}{(2a)^2}\int_{-a}^{a}\int_{-a}^{a} \frac{2/\pi}{\sqrt{1-(x/a)^2}} G(x, 0|nd + x', 0)\, dx' dx$$
$$\cong \begin{cases} \dfrac{1}{4i} H_n^{(2)}(k|n|d) & : n \neq 0 \\ \dfrac{1}{4i} - \dfrac{1}{2\pi}\left(\gamma + \ln\dfrac{ka}{4}\right) & \\ \quad - \left\{\dfrac{1}{4i} - \dfrac{1}{2\pi}\left(\gamma + \mathrm{In}\dfrac{ka}{4}\right) + \dfrac{1}{20\pi}\right\} \cdot \dfrac{5}{20}(ka)^2 & : n = 0 \end{cases} \tag{18}$$

$$S_1 = \sum_{\substack{n=-\infty \\ n\neq 0}}^{\infty} e^{-in\beta_o d} G_n \tag{19}$$

$$S_2 = \sum_{n=1}^{\infty} e^{-in\beta_o d} G_n \tag{20}$$

and $\gamma = 0.5772\cdots$ is Euler's constant. In the calculation of G_0, we have used the approximation of the Hankel function for small argument (see Eq. (A-8)) [15].

Equation (16) is an infinite set of equations to determine the unknown constants $\overline{J}^c_n$. Since $\overline{J}^c_n$ approaches zero as n increases

(see Eq. (5)), truncating Eq. (16) and solving it numerically, the unknown constants $\overline{J}_n^c$ can be determined. Here, we should note that the convergence of the series S_1 and S_2 is very slow and it is necessary to transform them into rapidly converging series. This can be done by using the Poisson's sum formula [16], and results are described in Appendix.

Note that this calculation method is equivalent to the Method of Moment in which the function $1/\sqrt{1-(x/a)^2}$ and the constant are used as the bases function and the weighting function, respectively.

3. FAR FIELD REPRESENTATION

Scattered field is expressed as follows:

$$E^s(x,y) = E^{s(p)}(x,y) + E^{s(c)}(x,y) \tag{21}$$

where $E^{s(p)}$ and $E^{s(c)}$ are the fields radiated by the currents J^p and J^c respectively, and $E^{s(p)}$ is called a "Kirchhoff solution" [10]. Referring to Eqs. (10), these fields are expressed as follows:

$$E^{s(p)}(x,y) = -i\omega\mu_0 \sum_{n=0}^{\infty} e^{-in\beta_0 d} \int_{-a}^{a} J^p(x') G(x,y\ |nd+x',0)\ dx' \tag{22}$$

$$E^{s(c)}(x,y) = -i\omega\mu_0 \sum_{n=0}^{\infty} \int_{-a}^{a} J^c(nd+x') G(x,y\ |nd+x',0)\ dx' \tag{23}$$

For convenience, let us transform Eqs. (22) and (23) into Fourier integral representations. Fourier transform and its inverse transform are defined by

$$\begin{cases} F(\zeta) = \displaystyle\int_{-\infty}^{\infty} f(x) e^{i\zeta x}\ dx \\ f(x) = \dfrac{1}{2\pi} \displaystyle\int_C F(\zeta) e^{-i\zeta x}\ d\zeta \end{cases} \tag{24}$$

where the contour C is the infinite paths in the complex ζ-plane as shown in Fig. 2(a). By using Eq. (24), we have

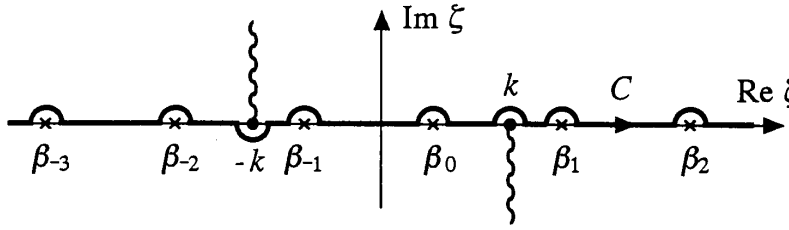

(a) contour C in complex ζ-plane

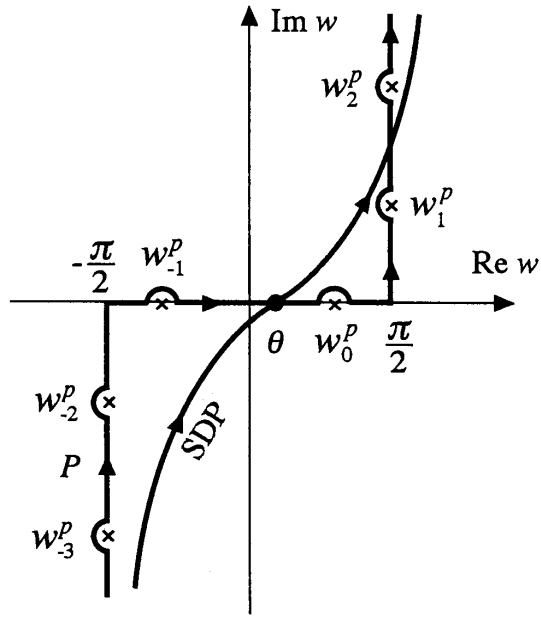

(b) contour P and SDP in complex w-plane

Figure 2. Paths of integration.

$$E^{s(p)}(x,y) = -\frac{\omega\mu_0 a\overline{J}^p}{2\pi}\int_C \frac{J_0(a\zeta)e^{\mp iy\sqrt{k^2-\zeta^2}}e^{-i\zeta x}}{\sqrt{k^2-\zeta^2}(1-e^{-i(\beta_0-\zeta)d})}d\zeta \quad (y \lessgtr 0) \tag{25}$$

$$E^{s(c)}(x,y) = -\frac{\omega\mu_0 a}{2\pi}\sum_{n=0}^{\infty}\overline{J}_n^c\int_C \frac{J_0(a\zeta)e^{\mp iy\sqrt{k^2-\zeta^2}}e^{-i(x-nd)\zeta}}{\sqrt{k^2-\zeta^2}}d\zeta \quad (y \lessgtr 0) \tag{26}$$

where J_0 is the zero-order Bessel function. Note that the integrand of Eq. (25) has poles at

$$\zeta = \beta_m = \beta_0 + 2m\pi/d \tag{27}$$

and these poles correspond to the Floquet's modes.

Next, in order to derive the far field representation, we evaluate the integrals of Eqs. (25) and (26) for $kr = k\sqrt{x^2+y^2} \gg 1$ by using the saddle point method [17]. Since the scattered field E^s is symmetric with respect to x-axis, we shall derive the far field representation for $|\theta| \leq \pi/2$. Let us introduce the following change of variables

$$\zeta = k\sin w, \qquad x = r\sin\theta, \qquad y = r\cos\theta. \tag{28}$$

By the above change of variables, the contour C of the integration is changed into P as shown in Fig. 2(b), and it can be deformed to the steepest descent path (SDP) which passes through the saddle point θ as shown in Fig. 2(b). As the results of the uniform asymptotic evaluation by the saddle point method [17], we have

$$E^s(r,\theta) = E^g(r,\theta) + E^d(r,\theta) \qquad r \to \infty \tag{29}$$

where

$$E^g(r,\theta) = -\frac{\omega\mu_0 a\overline{J}^p}{d}\sum_{[m]}\frac{J_0(\beta_m a)}{\sqrt{k^2-\beta_m^2}}e^{-ikr\cos(\theta-w_m^p)}u(\theta-w_m^p)$$

$$E^d(r,\theta) = -\frac{\omega\mu_0 a\overline{J}^p}{d}\sum_{[m]}\left[-\mathrm{sgn}(\theta - w_m^p)\frac{J_0(\beta_m a)}{\sqrt{k^2-\beta_m^2}}\right.$$
$$\left. e^{-ikr\cos(\theta - w_m^p)}\frac{e^{-i\pi/4}}{\sqrt{\pi}}\Phi(\zeta_m)\right] - \frac{\omega\mu_0 a}{2}\sqrt{\frac{2}{\pi kr}}e^{-i(kr-\pi/4)}$$
$$\left[\overline{J}^p\left\{\frac{J_0(ka\sin\theta)}{1-\exp[-ikd(\sin\theta_i - \sin\theta)]}\right.\right.$$
$$\left.\left. -\frac{i}{2d}\sum_{[m]}\frac{J_0(\beta_m a)}{\sqrt{k^2-\beta_m^2}}\frac{1}{\sin\left(\dfrac{\theta - w_m^p}{2}\right)}\right\}\right.$$
$$\left. +J_0(ka\sin\theta)\sum_{n=0}^{\infty}\overline{J}_n^c e^{inkd\sin\theta}\right]$$
$$\zeta_m = \sqrt{2kr}\sin\frac{|\theta - w_m^p|}{2}$$
$$\Phi(\xi) = \int_{\xi}^{\infty} e^{-it^2}\,dt$$
$$u(\theta) = \begin{cases} 1 \;:\; \theta > 0 \\ 0 \;:\; \theta < 0 \end{cases}$$

and $\sum_{[m]}$ is the summation over m for which $|\beta_m| < k$ holds, and w_n^p which are the poles satisfying the relation

$$k\sin w_m^p = \beta_m \tag{35}$$

correspond to the Floquet's modes of periodic structure. Eq. (29) indicates that the scattered field by a semi-infinite grating is expressed as a sum of two types of waves, E^g and E^d. The wave E^g, which is the residue contribution, is a set of plane waves (Floquet's modes) and E^d is a cylindrical wave diffracted at the end of the semi-infinite grating as shown in Fig. 3. It can be shown that the amplitudes and the directions of propagation of the plane waves of E^g coincide with those of Floquet's modes of the infinite grating shown in Fig. 1(b). It

is, however, found from Eq. (30) that they exist only within the region $w_m^p < \theta \leq \pi/2$. Therefore, the lines $\theta = w_m^p$ act as the shadow and reflection boundaries of the plane waves similar to those appearing in the diffraction by a conducting half plane. This result is also pointed out by Hills and Karp [10].

4. NUMERICAL RESULTS AND DISCUSSIONS

First, we shall show the currents on the strips. Fig. 4 shows the averaged current densities $\overline{J}_n^h$ and $\overline{J}_n^c$. In Fig. 4(c), log scale representation of $\overline{J}_n^c$ are also shown. From these figures, it can be found that the correction currents has, as we expected, a property of Eq. (5) and they act $\overline{J}_n^c \propto (knd)^{-3/2}$. Therefore, the behavior of $\overline{J}_n^h$ can be expressed as follows:

$$\overline{J}_n^h = \overline{J}^p e^{-in\beta_0 d} + O((knd)^{-3/2}) \tag{36}$$

Since the current on a conducting half plane J^{CHP} is expressed as

$$\begin{aligned} &J^{CHP}(kx) = J^{PO}(kx) + O((kx)^{-3/2}), \qquad kx \to \infty \\ &J^{PO} : \text{ Physical optics current} \end{aligned} \tag{37}$$

the current on a semi-infinite strip grating behaves similar to that on a conducting half plane.

Fig. 5 shows the diffracted fields E^d for narrow spacing $(d = 0.1\lambda)$. These patterns are normalized by one half of the intensity of the incident wave. For comparison, diffracted fields by a conducting half plane are also shown. Since $kd \ll 1$, diffraction patterns from a semi-infinite strip grating agree well with those from a conducting half plane. The Kirchhoff solution, which are obtained by letting $J^c = 0$, are also shown by the broken line. It is found from this result that the diffraction at $90°$ is suppressed by the effect of the correction currents.

Fig. 6 shows the diffracted fields for $d = 0.6\lambda$. We can find from this result that the diffraction patterns have sharp nulls that do not exist in Kirchhoff solutions. Hills and Karp [10] have analytically investigated the existence of these nulls, and have pointed out that these nulls appear in the direction of the propagation of the spatial harmonic waves for $\theta_i = 90°$, that is

$$\theta_{null} = \arctan \frac{\sqrt{k^2 - (k + 2m\pi/d)^2}}{k + 2m\pi/d} \ . \tag{38}$$

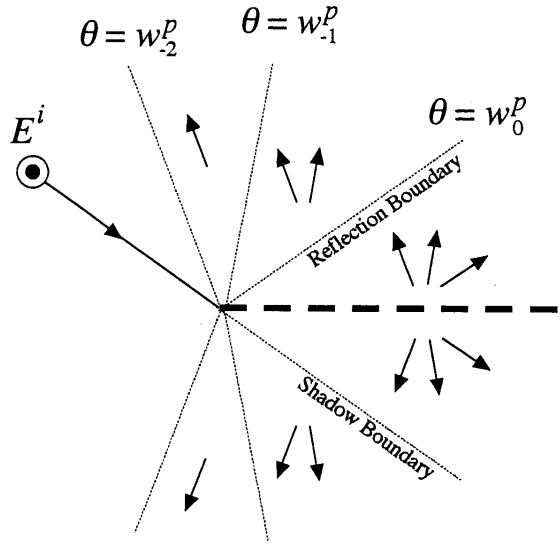

(a) Floquet's modes E^g

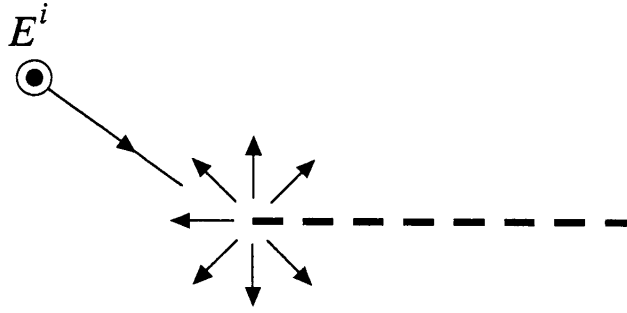

(b) edge diffracted wave E^d

Figure 3. Diffracted wave by a semi-infinite grating.

Although the above result by Hills and Karp is obtained under the restriction that the spacing of the elements is large relative to the wavelength, we can confirm from Fig. 6 that their result is true when the spacing is narrow.

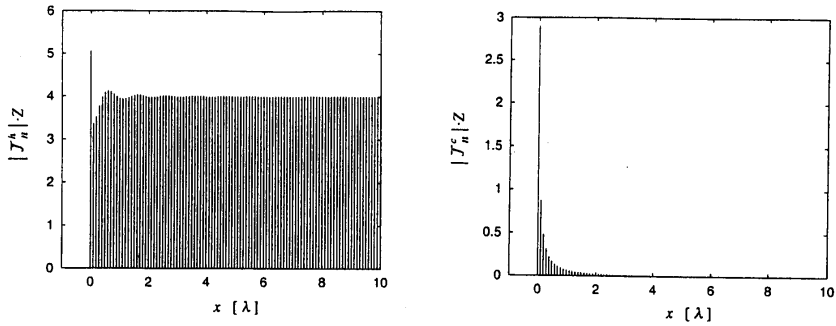

(a) $d = 0.1\lambda$

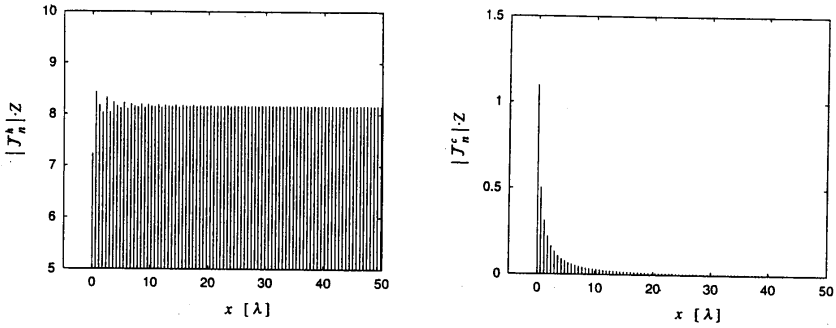

(b) $d = 0.6\lambda$

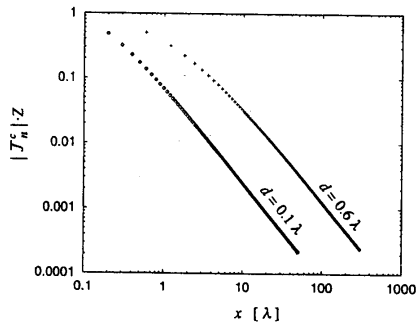

(c) log scale representation of $\overline{J}_n^c$.

Figure 4. Averaged current densities $\overline{J}_n^h$ and $\overline{J}_n^c$. ($2a = 0.05\lambda$, $\theta_i = 0^\circ$).

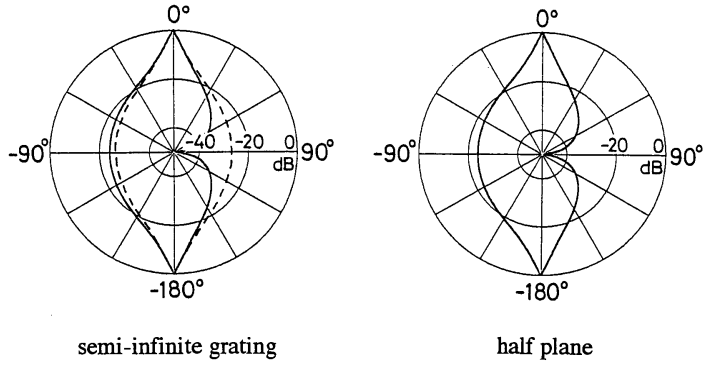

(a) $\theta_i = 0°$

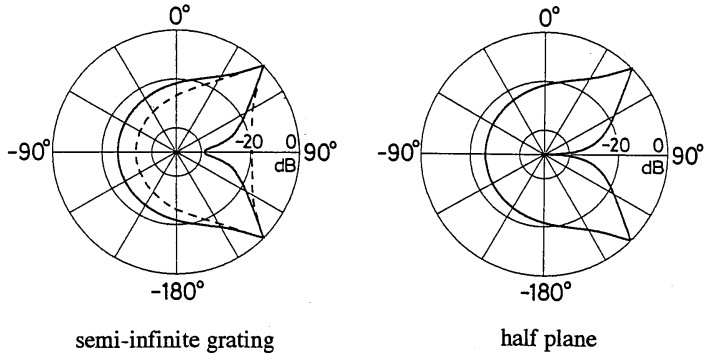

(b) $\theta_i = 45°$

Figure 5. Diffraction patterns for narrow spacing. ($2a = 0.05\lambda$, $d = 0.1\lambda$, $kr = 50\lambda$; ——: E^d, - - - -: Kirchhoff solution).

Finally, we shall quantitatively evaluate the end-effects contribution. The end-effects of the semi-infinite grating can be considered as the effects caused by the correction current J^c. Thus, in order to estimate the degree of the end-effects contribution, we calculate the radiated power W^c by J^c. The radiated power W^c is given by

$$W^c = \frac{1}{Z}\int_0^{2\pi} |E^{s(c)}(r,\theta)|^2 r d\theta, \qquad r \to \infty \tag{39}$$

where Z is a wave impedance in free space. Furthermore, we define

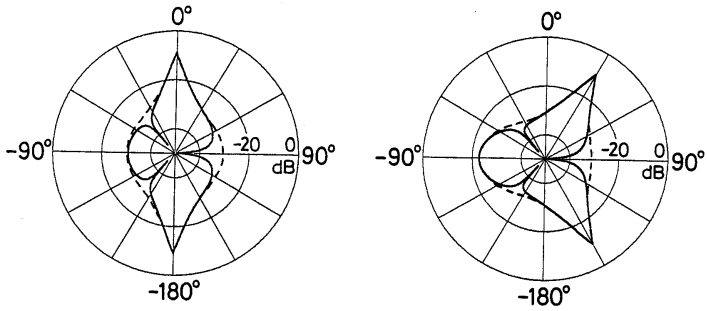

(a) $\theta_i = 0°$ **(b)** $\theta_i = 30°$

Figure 6. Diffraction patterns. ($2a = 0.05\lambda$, $d = 0.6\lambda$, $kr = 50\lambda$; ——: E^d, - - - -: Kirchhoff solution).

the normalized radiated power R as follows:

$$R = \frac{W^c}{2aP_{in}} \tag{40}$$

where P_{in} is the power density of the incident plane wave. Fig. 7 shows the normalized radiated power R versus the spacing d. We can find, from this figure, that R becomes large when $d = m\lambda$ for $\theta_i = 0°$ and $d = 0.586m\lambda$ for $\theta_i = -45°$ where $m = 1, 2, 3, \ldots$. For infinite grating, these values correspond to the spacing for cutoff of the m-th mode expressed as follows:

$$d = \frac{m}{\pm 1 - \sin\theta_i}\lambda \qquad (m = 1, 2, 3, \cdots) \tag{41}$$

Physically, above spacing corresponds to the condition for which the multiple scattering between the elements becomes strong (or the Wood's anomaly occurs). Therefore, this result indicates that the end-effect of the semi-infinite grating becomes large for cut-off frequencies.

5. CONCLUSIONS

In order to reveal the end-effects of the finite grating, we have analyzed the diffraction of electromagnetic waves by a semi-infinite strip grating under the assumption that the strip is narrow relative to the wavelength. Numerical results of current distributions and diffraction

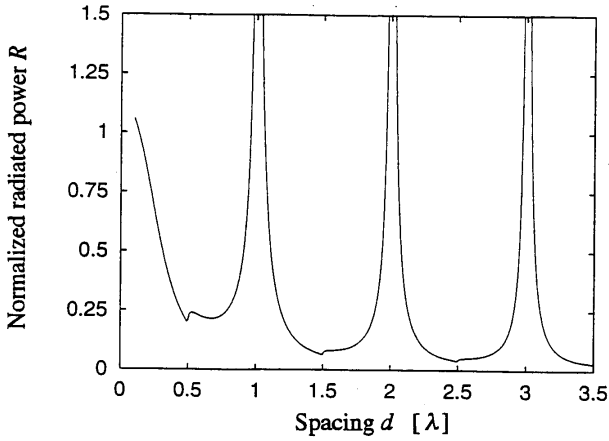

(a) $\theta_i = 0°$

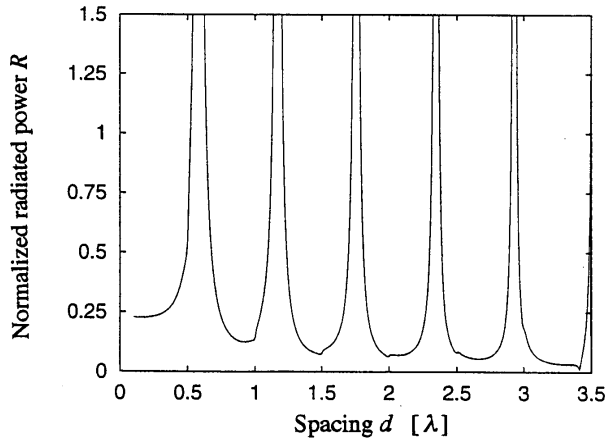

(b) $\theta_i = -45°$

Figure 7. Normalized radiated power R $(2a = 0.05\lambda)$. From Eq. (41), cut-off occurs at $d = \lambda,\ 2\lambda,\ 3\lambda, \ldots$ for $\theta_i = 0°$, and $d = 0.586\lambda,\ 1.172\lambda,\ 1.757\lambda,\ 2.343\lambda,\ 2.939\lambda,\ 3.414\lambda, \ldots$ for $\theta_i = -45°$.

patterns have revealed the behavior of the current near the edge and the existence of the sharp nulls in the diffraction patterns. It has also been found that the end-effects contribution becomes large for cutoff frequencies. These results are very useful for evaluating the diffraction by a strip grating of finite size. Furthermore, according to the concept of the GTD, we can easily obtain the diffraction coefficients

of semi-infinite grating from Eq. (31), and will be able to use them in calculating the diffraction by a strip grating of finite size.

In order to investigate the end-effects contribution in more detail, we have to calculate the near field around the edge and reveal the interaction between edge diffracted wave and Floquet's modes. This analysis is currently under investigation.

APPENDIX

A.1 Calculation of S_1

Since the series S_1 is rewritten as

$$S_1 = \frac{1}{4i} \lim_{\rho \to 0} \left[\sum_{n=-\infty}^{\infty} H_0^{(2)} \left(k\sqrt{\rho^2 + (nd)^2} \right) e^{in\beta_o d} - H_0^{(2)}(k\rho) \right] \quad \text{(A.1)}$$

we first calculate the following series

$$I = \sum_{n=-\infty}^{\infty} H_0^{(2)} \left(k\sqrt{\rho^2 + (nd)^2} \right) e^{in\beta_o d}. \quad \text{(A.2)}$$

By using the Poisson's sum formula [16] and the following Fourier transform of Hankel function

$$\int_{-\infty}^{\infty} H_0^{(2)}(\sqrt{\rho^2 + x^2}) e^{i\zeta x}\, dx = 2\frac{\exp\left[-i\rho\sqrt{k^2 - \zeta^2}\right]}{\sqrt{k^2 - \zeta^2}} \quad \text{(A.3)}$$

Eq. (A.2) is transformed into spectral domain series

$$I = \frac{2}{d} \sum_{n=-\infty}^{\infty} \frac{\exp\left[-i\rho\sqrt{k^2 - \beta_n^2}\right]}{\sqrt{k^2 - \beta_n^2}} \quad \text{(A.4)}$$

where the branch of $\sqrt{k^2 - \beta_n^2}$ should be chosen so that the series of Eq. (A.4) converges: that is

$$\sqrt{k^2 - \beta_n^2} = \begin{cases} \sqrt{k^2 - \beta_n^2} & : \quad k^2 > \beta_n^2 \\ -i\sqrt{\beta_n^2 - k^2} & : \quad k^2 < \beta_n^2 \end{cases}. \quad \text{(A.5)}$$

In order to improve the convergence of the series I, we introduce the formula of logarithmic series

$$\sum_{n=1}^{\infty} \frac{\exp[-i\rho(2n\pi/d)]}{-i(2n\pi/d)} = \frac{d}{2\pi i} \ln(1 - \exp[-2\pi\rho/d]). \tag{A.6}$$

Thus, Eq. (A.4) is rewritten as follows:

$$\begin{aligned} I = 2/d \sum_{n=1}^{\infty} \Bigg\{ & \frac{\exp\left[-i\rho\sqrt{k^2-\beta_n^2}\right]}{\sqrt{k^2-\beta_n^2}} + \frac{\exp\left[-i\rho\sqrt{k^2-\beta_{-n}^2}\right]}{\sqrt{k^2-\beta_{-n}^2}} \\ & - \frac{id}{n\pi} \exp[-i\rho(2n\pi/d)] \Bigg\} + \frac{2}{i\pi} \ln(1 - \exp[-2\pi\rho/d]) \\ & + \frac{2}{d} \frac{\exp\left[-i\rho\sqrt{k^2-\beta_0^2}\right]}{\sqrt{k^2-\beta_0^2}} \end{aligned} \tag{A.7}$$

By using the above series and the approximation of Hankel function for small argument [15]

$$H_o^{(2)}(k\rho) \cong \left(1 - \frac{2i}{\pi}(\gamma + \ln\frac{k\rho}{2})\right)\left(1 - \frac{(k\rho)^2}{4}\right) - \frac{i(k\rho)^2}{2\pi} \tag{A.8}$$

the series S_1 of Eq. (A.1) is transformed into following series that converges rapidly

$$\begin{aligned} S_1 = & \frac{1}{2\pi}\left(\gamma + \ln\frac{kd}{4\pi}\right) + i\left(\frac{1}{4} - \frac{1}{2d}\frac{1}{\sqrt{k^2-\beta_0^2}}\right) \\ & + \frac{1}{2id}\sum_{n=1}^{\infty}\left\{\frac{1}{\sqrt{k^2-\beta_n^2}} + \frac{1}{\sqrt{k^2-\beta_{-n}^2}} - \frac{id}{n\pi}\right\} \end{aligned} \tag{A.9}$$

A.2 Calculation of S_2

Series S_2 can be transformed into rapidly converging series in the same manner for S_1. Rewriting the series S_2 in the following form

$$\begin{aligned} S_2 &= \frac{1}{4i}\sum_{n=1}^{\infty} H_0^{(2)}(knd)e^{-in\beta_0 d} \\ &= \frac{1}{8i}\sum_{\substack{n=\infty \\ n\neq 0}}^{\infty} H_0^{(2)}(k|n|d)e^{-i|n|\beta_0 d} \\ &= \frac{1}{8i}\lim_{\rho\to 0}\left[\sum_{n=-\infty}^{\infty} H_0^{(2)}\left(k\sqrt{\rho^2+(nd)^2}\right)e^{-i|n|\beta_0 d} - H_0^{(2)}(k\rho)\right] \end{aligned} \tag{A.10}$$

and applying the same procedure for deriving Eq. (A.9), S_2 can be transformed into series that converges rapidly. As the final result, we get

$$\begin{aligned} S_2 = \frac{1}{4\pi}\left(\gamma + \ln\frac{kd}{4\pi}\right) - \frac{1}{8i}\left[1 - \frac{2}{d}\frac{1-\frac{2}{\pi}\arcsin\left(\frac{\beta_0}{k}\right)}{\sqrt{k^2-\beta_0^2}}\right] \\ + \frac{1}{4id}\sum_{n=1}^{\infty}\left[\frac{1-\frac{2}{\pi}\arcsin\left(\frac{\beta_n}{k}\right)}{\sqrt{k^2-\beta_n^2}} + \frac{1-\frac{2}{\pi}\arcsin\left(\frac{\beta_{-n}}{k}\right)}{\sqrt{k^2-\beta_{-n}^2}} - \frac{id}{n\pi}\right] \end{aligned} \tag{A.11}$$

where the branch of the arc sine is defined as follows:

$$\arcsin\zeta = \begin{cases} \arcsin\zeta & : \ |\zeta| < 1 \\ \dfrac{\pi}{2} - i\ln(\zeta - \sqrt{\zeta^2-1}) & : \ \zeta > 1 \\ -\dfrac{\pi}{2} + i\ln(-\zeta - \sqrt{\zeta^2-1}) & : \ \zeta < -1 \end{cases} \tag{A.12}$$

REFERENCES

1. Zaki, K. A. and A. R. Nuereuther, "Scattering from a perfectly conducting surface with a sinusoidal height profile: TE polarization," *IEEE Trans. Antennas & Propagat.,* Vol. AP-19, 208–214, 1971.
2. Ikuno, H. and K. Yasuura, "Improved point matching method with application to scattering from a periodic surface," *IEEE Trans.,* Vol. AP-21, No. 5, 657–662, 1973.
3. Petit, R. Ed., "Electromagnetic theory of gratings," *Series topics in current physics,* Springer Verlag, New York, 1980.
4. Uchida, K., T. Noda, and T. Matsunaga, "Spectral domain analysis of electromagnetic wave scattering by an infinite plane metallic grating," *IEEE Trans. Antennas & Propagat.,* Vol. AP35, No. 1, 46–52, 1987.
5. Twelsky, V., "On a multiple scattering theory of the finite grating and Wood's anomalies," *J. Appl. Phys.,* Vol. 23, No. 10, 1099–1118, 1952.
6. Ko, W. L. and R. Mittra, "Scattering by a truncated periodic array," *IEEE Trans. Antennas & Propagat.,* Vol. AP-36, No. 4, 496–503, 1988.
7. Kobayashi, K. and T. Eizawa, "Plane wave diffraction by a finite sinusoidal grating," *Trans. IEICE,* Vol. E74, No. 9, 2815–2826, 1991.
8. Carin, L. and L. B. Felsen, "Time-harmonic and transient scattering by finite periodic flat strip arrays: Hybrid (Ray)–(Floquet Mode)–(MOM) algorithm and its GTD interpretation," *IEEE Trans. Antennas & Propagat.,* Vol. AP-41, No. 4, 412–421, 1993.
9. Usoff, J. M. and B. A. Munk, "Edge effects of truncated periodic surfaces of thin wire elements," *IEEE Trans. Antennas & Propagat.,* Vol. AP-42, No. 7, 946–953, 1994.
10. Hills, N. L. and S. N. Karp, "Semi-infinite diffraction gratings I and II," *Commu. Pure Appl. Math.,* Vol. 18, 203–233, 389–398, 1965.
11. Mittra, R., C. H. Chan, and T. Cwik, "Techniques for analyzing frequency selective surfaces - A Review," *Proc. IEEE,* Vol. 76, No. 12, 1593–1615, 1988.
12. Ando, M., A. Kondo, and K. Kagoshima, "Scattering of an arbitrary wave by a thin strip grating reflector," *IEE Proc.,* Vol. 133, No. 3, 203–208, 1986.
13. Ando, M. and K. Takei, "Reflection and transmission coefficients of a thin strip grating for antenna application," *IEEE Trans. Antennas & Propagat.,* Vol. AP-35, No. 4, 367–371, 1987.

14. Nishimoto, M. and K. Aoki, "Scattering of plane electromagnetic wave by a semi-infinite strip grating," *Trans. IECE of Japan,* Vol. E69, No. 11, 1161–1164, 1986.
15. Jones, D. S., *Acoustic and Electromagnetic Waves,* 672, Clarendon Press, Oxford, 1986.
16. Morse, P. H. and H. Feshbach, *Method of Theoretical Physics,* McGraw-Hill, 466–467, 1953.
17. Felsen, L. B. and N. Marcuvits, *Radiation and Scattering of Waves,* Chap. 4, Prentice-Hall, 1973.